



## RESEARCH ARTICLE

Biomolecular Engineering, Bioengineering, Biochemicals, Biofuels, and Food

# Engineering a drug eluting ocular patch for delivery and sustained release of anti-inflammatory therapeutics

Xi Chen<sup>1</sup> | Shima Gholizadeh<sup>1</sup> | Mahsa Ghovvati<sup>1</sup>  | Ziqing Wang<sup>1</sup> |  
Marcus J. Jellen<sup>2</sup> | Azadeh Mostafavi<sup>1</sup> | Reza Dana<sup>3</sup> | Nasim Annabi<sup>1,4</sup> <sup>1</sup>Department of Chemical and Biomolecular Engineering, University of California – Los Angeles, Los Angeles, California, USA<sup>2</sup>Department of Chemistry and Biochemistry, University of California – Los Angeles, Los Angeles, California, USA<sup>3</sup>Schepens Eye Research Institute, Mass Eye and Ear, Department of Ophthalmology, Harvard Medical School, Boston, Massachusetts, USA<sup>4</sup>Department of Bioengineering, University of California – Los Angeles, Los Angeles, California, USA**Correspondence**

Nasim Annabi, Department of Chemical and Biomolecular Engineering, University of California – Los Angeles, Los Angeles, CA, USA.

Email: [nannabi@ucla.edu](mailto:nannabi@ucla.edu)**Funding information**

National Institute of Biomedical Imaging and Bioengineering, Grant/Award Number: R01EB023052; U.S. Army Medical Research Institute of Chemical Defense, Grant/Award Number: W81XWH-21-1-0869; Department of Defense Vision Research Program Technology/Investigator-Initiated Research Award; National Institutes of Health

**Abstract**

Ocular inflammation is commonly associated with eye disease or injury. Effective and sustained ocular delivery of therapeutics remains a challenge due to the eye physiology and structural barriers. Herein, we engineered a photocrosslinkable adhesive patch (GelPatch) incorporated with micelles (MCs) loaded with loteprednol etabonate (LE) for delivery and sustained release of drug. The engineered drug loaded adhesive hydrogel, with controlled physical properties, provided a matrix with high adhesion to the ocular surfaces. The incorporation of MCs within the GelPatch enabled solubilization of LE and its sustained release within 15 days. *In vitro* studies showed that MC loaded GelPatch supported cell viability and growth. In addition, subcutaneous implantation of the MC loaded GelPatch in rats confirmed its *in vivo* biocompatibility and stability within 28 days. This non-invasive, adhesive, and biocompatible drug eluting patch can be used as a matrix for the delivery and sustained release of hydrophobic drugs.

**KEYWORDS**

anti-inflammatory, controlled drug delivery, micelles, ocular injuries, release

## 1 | INTRODUCTION

Continuous and efficient delivery of anti-inflammatory therapeutics into inflamed ocular tissues can be a challenge, in part due to patient compliance as well as structural barriers in the eye. Additionally, systemic administration routes require a large dose in order to achieve a satisfactory drug concentration at the ocular tissue, which can lead to off-target systemic side effects.<sup>1</sup> On the other hand, local drug delivery systems such as the conventional topical administration (eye drops or ointments) have extremely low bioavailability of <5% due to the

corneal epithelium barrier and fast clearance by tear film and blinking.<sup>2</sup> Intraocular injection can be used to circumvent some of these challenges, including bioavailability issues,<sup>3</sup> but this method is also invasive and may be associated with certain complications such as pain, intraocular pressure spikes, among others.<sup>4</sup> Hence, a local technology that is non-invasive while permitting sustained drug delivery is highly preferred.

Various patch-based drug delivery systems based on different polymers have been developed throughout the years, yet there are several shortcomings with so far developed ocular patches as drug delivery platforms. For example, drug-eluting soft contact lenses (SCL) made of silicone polymers were successfully engineered.<sup>5</sup> SCL have

Xi Chen and Shima Gholizadeh contributed equally to this work.

been loaded with drugs either by soaking them in a concentrated drug solution or by incorporating liposomes containing drug molecules via multilayer immobilization and surface modifications. However, drawbacks associated with these post-modifying SCL have been sub-optimal drug loading and occasionally issues with optical transparency and wettability.<sup>6,7</sup> Although these SCLs were designed to have good oxygen permeabilities, yet their long-term application (e.g., more than 8 h) with constant eye movement could induce irritation and inflammation.

To address this need, we envisioned the unmet need to develop a drug loaded adhesive patch as a platform technology for sustained release of therapeutics with improved bioavailability compared to conventional eye drops. Using biocompatible and biodegradable materials can further improve the patient's life quality and the cost by reducing hospital visits for patch removal. There are several types of ocular adhesive patches developed so far with high adhesion to ocular tissues, but these platforms have mainly focused on sealing and repair of ocular injuries without incorporating a sustained drug delivery system.<sup>8,9</sup> For example, cyanoacrylate-based ocular adhesives are sometimes used by ophthalmologists to seal eye wounds.<sup>8,9</sup> Although cyanoacrylate-based adhesives could offer a fast and easy sealing ocular injuries, they are associated with several drawbacks including cytotoxicity, irregular rough surfaces, and nonbiodegradable nature.<sup>9</sup> In addition, they are not designed to elute drugs. Poly(ethylene glycol) (PEG)-based ocular glues, on the other hand, are biocompatible and have tunable mechanical properties and biodegradability.<sup>10–12</sup> For instance, ReSure, a PEG-based adhesive, is a Food and Drug Administration (FDA)-approved ocular sealant used to seal corneal incisions upon cataract surgery.<sup>13</sup> However, ReSure requires a mixing of two components and only allows a 14–17 s application time window after mixing, which can be limited in some circumstances.<sup>14</sup> Moreover, fibrin sealant, a naturally derived polymer-based ocular adhesive, shows excellent biocompatibility and biodegradability but it requires a longer gelation time after application and has lower adhesive strength specially to wet surfaces.<sup>15</sup>

Our team has recently developed a photocrosslinkable gelatin-based adhesive hydrogel based on gelatin methacryloyl (GelMA), which showed high biocompatibility with strong adhesion to corneal stromal defects. Before crosslinking, GelMA remains in a liquid form to be applied directly on stromal defect, but it does not provide enough viscosity to retain onto the intact cornea surfaces.<sup>16</sup> Hyaluronic acid (HA) is known as a viscoelastic and highly biocompatible glycosaminoglycan.<sup>17</sup> By modifying HA with photocrosslinkable groups and mixing it with GelMA and Poly(ethylene glycol) diacrylate (PEGDA) at a specific weight ratio, we engineered GelPatch composite adhesives with improved physical properties.<sup>17</sup> GelPatch prepolymers showed high wet surface retention (preferred viscosity) before photocrosslinking and strong tissue adhesion and mechanical properties after photocrosslinking to be used as a matrix for ocular drug delivery. The high adhesion and biocompatibility of GelPatch can provide a great potential to circumvent the drawbacks of contact lens, microneedle patches, and other currently available adhesives in the market. In this work, we loaded micelle- solubilized anti-

inflammatory drugs into GelPatch and investigated the sustained release profile of the drugs from these patches for treatment of ocular complications.

Topical corticosteroids are commonly used in the treatment of ocular anterior segment diseases and postoperative inflammation due to their anti-inflammatory effects.<sup>18</sup> Loteprednol etabonate (LE), prednisolone acetate (PA), and dexamethasone (DEX) are three examples of corticosteroids with established safety profiles, which have been used for the treatment of ocular inflammatory diseases. Since corticosteroids are hydrophobic drugs with poor solubility in water, it is desired to solubilize them before loading into hydrogel patches. To address this issue, the encapsulation of hydrophobic drugs in nanocarriers has widely been described.<sup>2,19,20</sup> The desired drug carrier should be small, surface hydrophilic, and net-neutral surface charge in order to be incorporated into hydrogel patches. In addition, the drug carrier should also have a hydrophobic core to load hydrophobic drugs and enable sustained drug release. Polymeric micelles (MCs) consisting of a hydrophilic shell and a hydrophobic core are excellent candidates to deliver hydrophobic drugs.<sup>21,22</sup> Several polymeric MC-based ocular drug delivery systems with sustained release profiles have been reported recently.<sup>23,24</sup> Biodegradable poly(ethylene glycol)-b-poly[N-(2-hydroxypropyl) methacrylamide-lactate] (mPEG-b-p(HPMAm-Lac)<sub>n</sub>) diblock copolymers have been successfully used to deliver hydrophobic drugs for cancer therapy,<sup>25,26</sup> but their use for the encapsulation of corticosteroids for ocular drug delivery has not been studied yet.

The aim of this study is to develop anti-inflammatory drug eluting patches which facilitate drug penetrating through the structural barriers of ocular tissues by adhering to the ocular surface and providing a sustained release of drugs directly to the injured sites. Corticosteroids play a prominent role in the therapeutic management of chronic ocular anterior segment inflammation.<sup>27</sup> The three drug molecules selected for this study were LE, PA, DEX. All three drug molecules are lipophilic (LogP > 0) with minor differences in their molecular structures and overall poor water solubility (<0.1 mg/mL).<sup>28</sup> Among these three compounds, LE has only one H-bond donor and the highest LogP (LogP = 3.08), which explains its lowest solubility in water (0.0005 mg/mL).<sup>28</sup> We solubilized the three selected drug molecules in mPEG-b-p(HPMAm-Lac)<sub>n</sub> polymeric MCs and compared the micellar size, drug loading efficiency, and sustained drug release profiles. The optimized MC formulations were then loaded inside GelPatch to form drug eluting adhesives for treatment of eye inflammation. The engineered GelPatch was optimized at both liquid and solid states for high ocular retention upon instillation, and post crosslinking adhesion, swelling ratio, and mechanical properties while retaining high *in vitro* and *in vivo* cytocompatibility.<sup>17</sup> The physical properties of the engineered drug loaded patches were assessed by performing swelling study, burst pressure and mechanical tests. *In vitro* release profiles with and without the presence of enzymes were also assessed. Lastly, *in vivo* tests were conducted using a rat subcutaneous implantation model to study the biocompatibility and biodegradation of the MC loaded GelPatch adhesives.

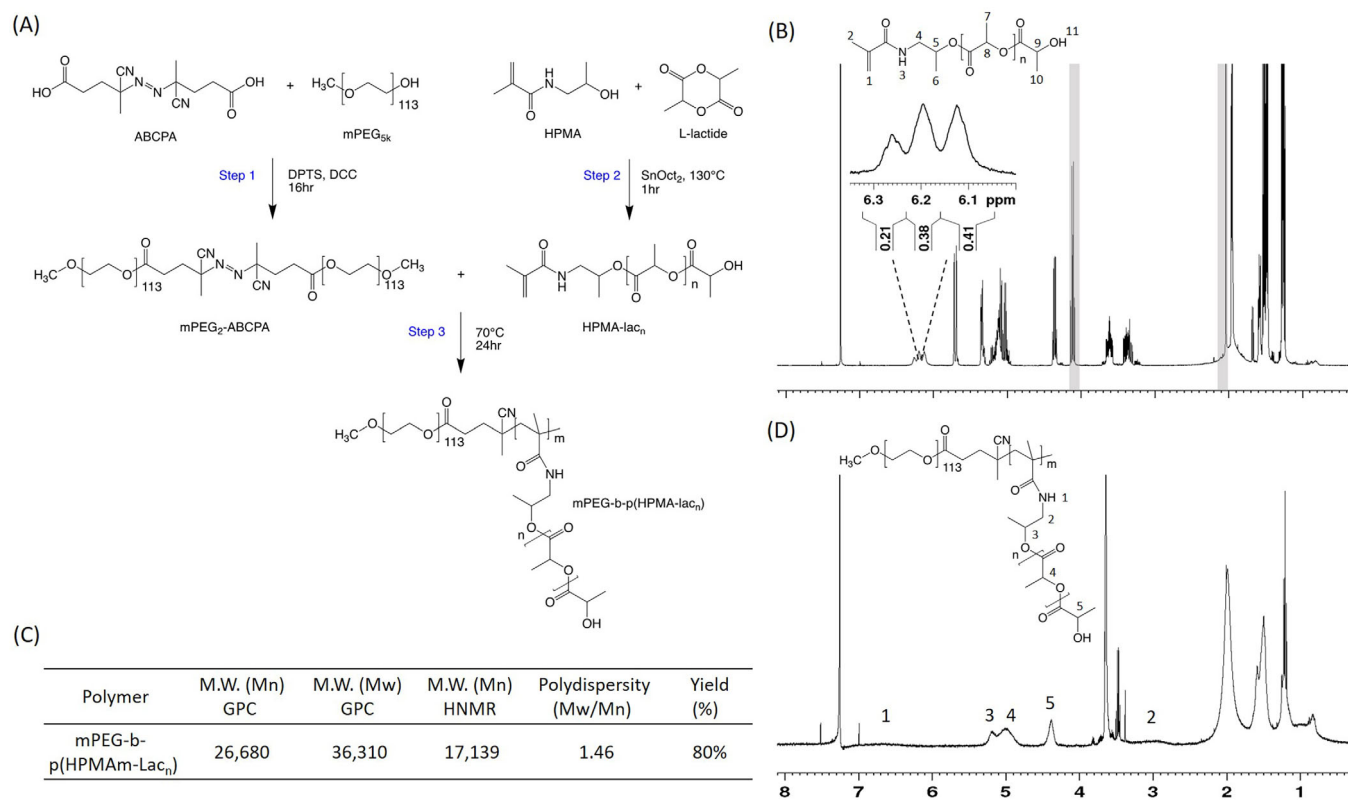


**FIGURE 1** Synthesis and characterization of mPEG-b-p(HPMAm-Lac<sub>n</sub>) copolymer. (A) A three-step synthetic scheme of mPEG-b-p(HPMAm-Lac<sub>n</sub>) copolymer. (B) <sup>1</sup>H NMR spectrum of HPMAm-Lac<sub>n</sub> monomer (—NH— peak is zoomed in). (C) Yield, GPC and <sup>1</sup>H NMR characterizations of copolymer: the number average molecular weight (*M<sub>n</sub>*), the weight average molecular weight (*M<sub>w</sub>*), polydispersity (*M<sub>w</sub>/M<sub>n</sub>*). (D) <sup>1</sup>H NMR spectrum of mPEG-b-p(HPMAm-Lac<sub>n</sub>) copolymer.

## 2 | RESULTS

### 2.1 | Synthesis and characterization of copolymer for MC formation

Diblock copolymer mPEG-b-p(HPMAm-Lac<sub>n</sub>) composed of a hydrophobic N-(2-hydroxypropyl)methacrylamide-lactate (HPMAm-Lac<sub>n</sub>) block and a hydrophilic methoxy poly(ethylene glycol) (mPEG) block was synthesized by radical polymerization with macroinitiator methoxy poly(ethylene glycol)<sub>2</sub>-azobis(4-cyanopentanoic acid) (mPEG<sub>2</sub>-ABCPA) in a high yield of 80% based on the procedure explained previously<sup>29</sup> (Figure 1A). Firstly, the monomer HPMAm-Lac<sub>n</sub> was synthesized by ring-opening oligomerization of L-lactide using SnOct<sub>2</sub> as a catalyst.<sup>30</sup> The monomer mixtures were purified through silica column chromatography to remove residual HPMAm and obtain a mixture of HPMAm-Lac<sub>2</sub> to HPMAm-Lac<sub>4</sub> in a form of light-yellow colored viscous solution. From proton nuclear magnetic resonance (<sup>1</sup>H NMR) spectrum, the percentage of HPMAm-Lac<sub>2</sub>, HPMAm-Lac<sub>3</sub> and HPMAm-Lac<sub>4</sub> were calculated to be 41%, 38%, and 21%, respectively, based on the integration ratio of amide protons (—NH—) in 6.1 ~ 6.3 ppm region (Figure 1B). In addition, the poly dispersity index (PDI) (*M<sub>w</sub>/M<sub>n</sub>*) of the copolymer was measured to be 1.46 based on gel permeation chromatography (GPC) analysis (Figure 1C), which was within the

expected range for the polymers synthesized via free radical polymerization.<sup>29</sup>

At the second step, mPEG<sub>2</sub>-ABCPA macroinitiator was synthesized. The <sup>1</sup>H NMR analysis confirmed the synthesis of mPEG<sub>2</sub>-ABCPA with a yield of ~90% (Figure S1). At the last step, the monomer was reacted with macroinitiator to obtain the final diblock copolymer. The average number of repeating units of HPMAm-Lac<sub>n</sub> was calculated to be ~32 (Equation 2), and therefore by adding the mPEG block, the average molecular weight of the synthesized block copolymer was calculated to be ~17,139 Da based on the <sup>1</sup>H NMR spectrum (Figure 1D). The synthesized mPEG-b-p(HPMAm-Lac<sub>n</sub>) block copolymers were then used as building blocks to form MCs, which will be used to solubilize our selected anti-inflammatory drugs.

### 2.2 | MC formation and its core interaction with corticosteroids

In previous studies, mPEG-b-p(HPMAm-Lac<sub>n</sub>) MCs were successfully synthesized and used to solubilize several hydrophobic therapeutics, such as paclitaxel and vitamin K, and an MRI contrast agent.<sup>25,26,31</sup> mPEG-b-p(HPMAm-Lac<sub>n</sub>) MCs were shown to have tunable biodegradability due to the hydrolysis of the lactate side chains under physiological conditions, which enabled sustained release of loaded

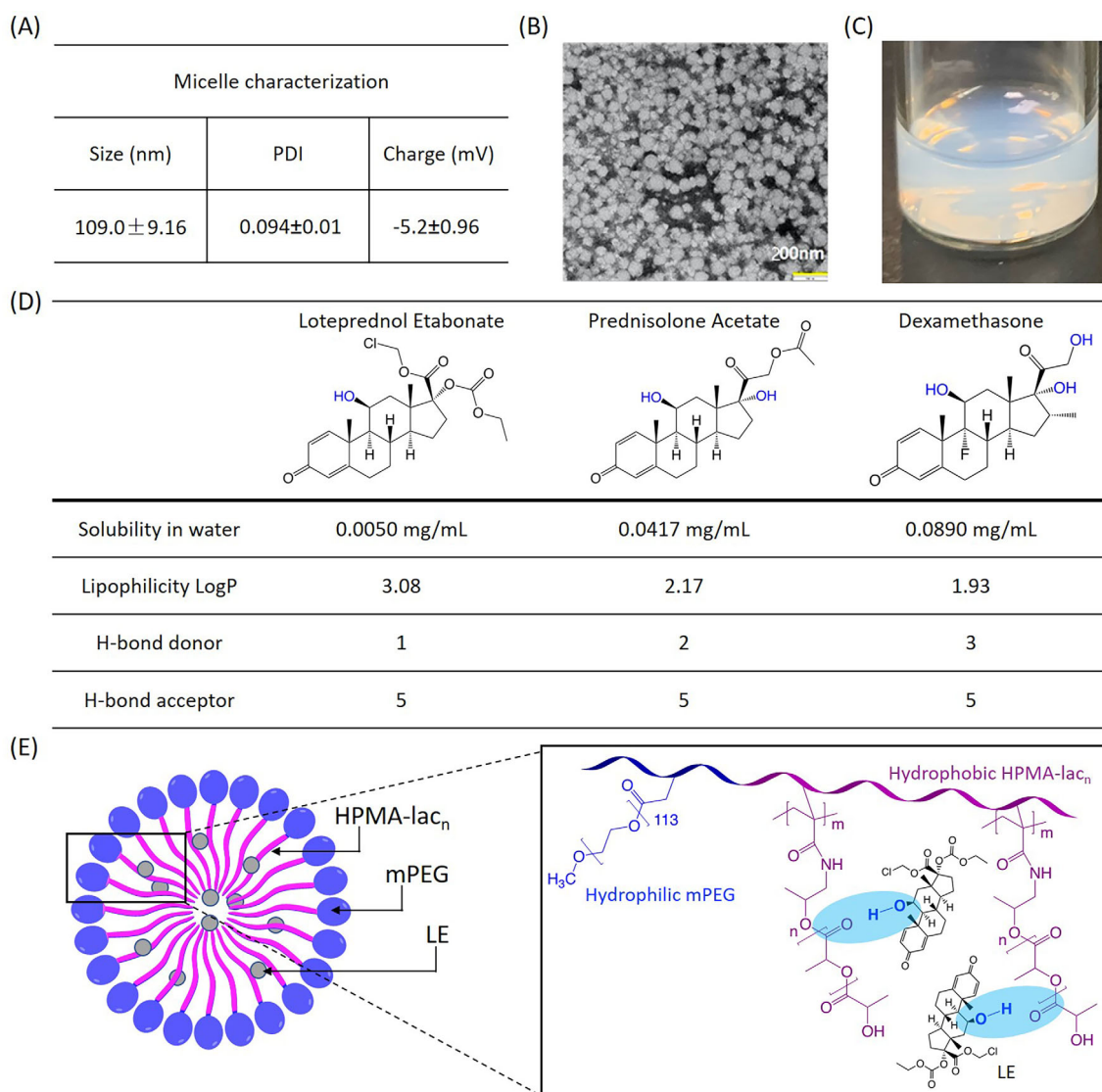


**FIGURE 2** Micelle formation and characterization. (A) The size (nm), PDI, and surface charge (mV) characterization of unloaded mPEG-b-p (HPMAm-Lac<sub>n</sub>) MCs. (B) A representative TEM image of unloaded MCs (scale bar, 200 nm). (C) Physical appearance of the solution of LE loaded MCs (copolymer/drug ratio (w/w) = 10:1). (D) The physical properties (solubility in water, lipophilicity LogP, donor and acceptor) and structures of three corticosteroids: LE, PA, and DEX. (E) A schematic of LE loaded MCs with drug and copolymer interaction shown in the box.

therapeutics via diffusion.<sup>32</sup> In addition, PEG shell of MCs offered several advantages including drug protection, prolonged systemic circulation, and reduced macrophage uptake. Their small size allowed better tissue penetration via enhanced permeability and retention (EPR) to overcome physiological barriers.<sup>25,26</sup> The engineered MCs were mainly used for cancer therapy.<sup>26,29</sup> Herein, for the first time, we utilized mPEG-b-p(HPMAm-Lac<sub>n</sub>) MCs to solubilize hydrophobic anti-inflammatory drugs for the treatment of ocular injuries.

MCs were formed by self-assembly via a solvent evaporation method.<sup>29</sup> mPEG-b-p(HPMAm-Lac<sub>n</sub>) copolymers were firstly dissolved in acetone and were fast added to an aqueous solution composed of ammonium acetate buffer solution. During the evaporation of acetone, amphiphilic copolymers formed core-shell structures with hydrophobic HPMAm-Lac<sub>n</sub> block clustering away from aqueous phase

and hydrophilic mPEG orienting toward aqueous phase.<sup>31</sup> The average size of unloaded MCs was 109.0 ± 9.16 nm with a PDI of 0.094 ± 0.01 measured by dynamic light scattering (DLS) (Figure 2A). The surface charge density of unloaded MCs was determined to be -5.2 ± 0.96 mV via Zetasizer. A representative transmission electron microscopy (TEM) image of unloaded MCs is shown in Figure 2B. The dispersion of formed MCs based on mPEG-b-p(HPMAm-Lac<sub>n</sub>) was opalescent and homogeneous (Figure 2C).

Figure 2D summarizes the physicochemical properties and molecular structure of three types of corticosteroids that were formulated within the synthesized MCs. LE, PA, and DEX are FDA-approved anti-inflammatory compounds, which are used to treat ocular anterior segment diseases.<sup>27</sup> They all have similar core structures with different functional groups attached to the cyclopentane ring in addition to a

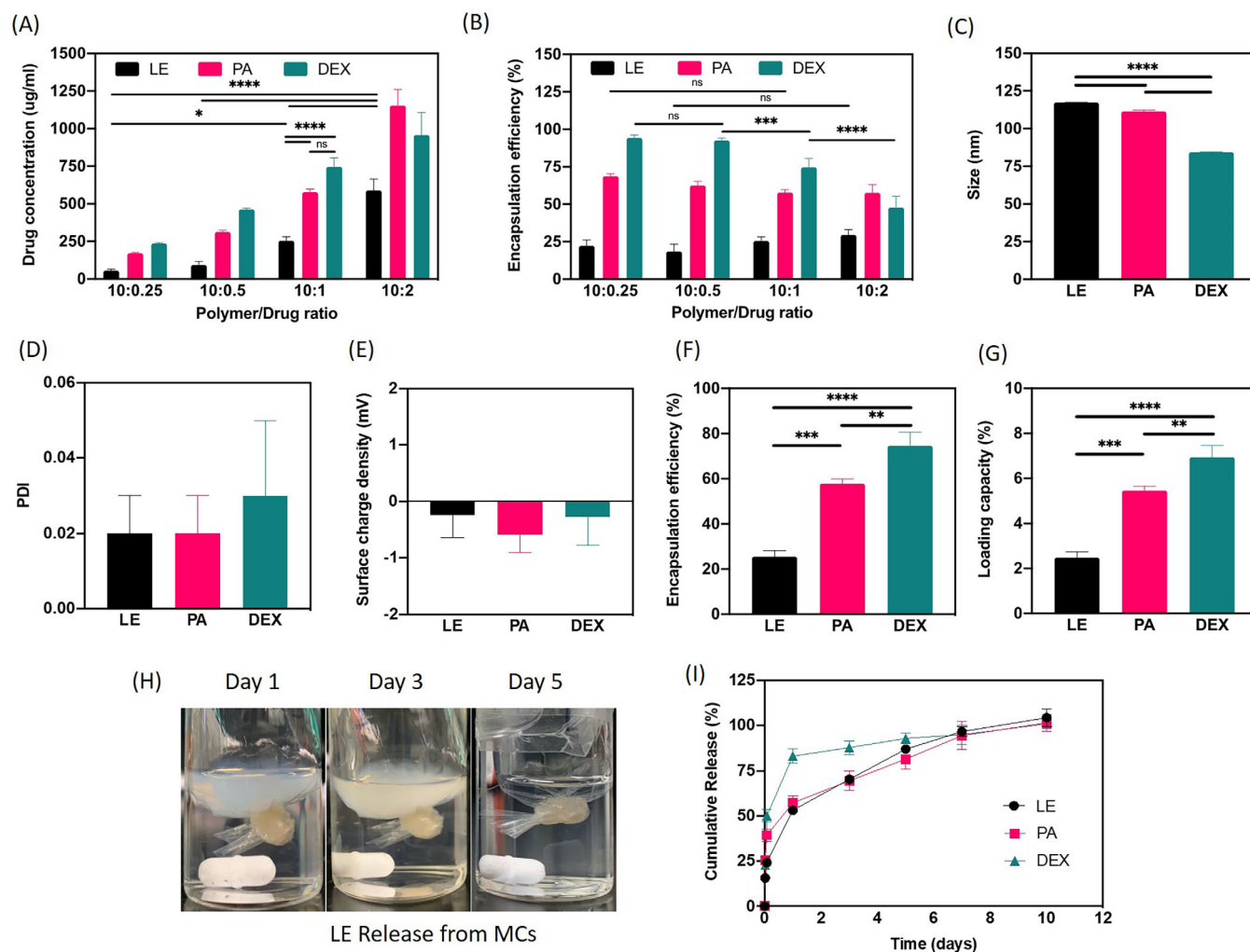


**FIGURE 3** Characterization of drug loaded MCs. (A) The concentrations of drugs (LE, PA, and DEX) in 1 mL of MC solution with different initial copolymer/drug ratios (w/w, 10:0.25, 10:0.5, 10:1, and 10:2). (B) Encapsulation efficiency (EE) for lomeperidone (LE), prednisolone acetate (PA) and dexamethasone (DEX) with different initial copolymer/drug ratios (w/w, 10:0.25, 10:0.5, 10:1, and 10:2). (C) The size (nm) measurements, (D) PDI, (E) surface charge (mV), (F) EE, and (G) loading efficiency (LC) for LE, PA and DEX loaded MCs at the initial copolymer/drug ratio of 10:1. (H) The appearance of LE loaded MCs in the dialysis bag immersed in the releasing medium of 2% Triton X-100 in DPBS at 37°C on days 1, 3, and 5. (I) Cumulative release of LE, PA, and DEX from the mPEG-b-p(HPMAM-Lac<sub>n</sub>) MCs at 37°C in a releasing medium containing 2% Triton X-100 in DPBS measured by HPLC at different time points (30 min, 2 h, 1 day, 3 days, 5 days, 7 days, and 10 days). Data is represented as means ± SD (\**p* < 0.1, \*\**p* < 0.01, \*\*\**p* < 0.001, \*\*\*\**p* < 0.0001).

fluoride at the carbon 9 (C-9) position for DEX and a hydrogen at C-9 position for LE and PA.<sup>18</sup> All three drug molecules are lipophilic (LogP > 0) with poor water solubility (<0.1 mg/mL). Among these three compounds, LE has only one H-bond donor and the highest LogP (LogP = 3.08), which explains its lowest solubility in water (0.0005 mg/mL).

Drug loaded MCs were formed by an additional step of mixing drugs with the synthesized copolymers in acetone before encountering with the aqueous phase. During the process of acetone evaporation, free floating hydrophobic drugs were slowly clustered with the hydrophobic blocks of copolymers to form the drug loaded MCs. Drug loading was achieved via both H-bonding and hydrophobic interactions between the drugs and copolymers functional groups (Figure 2E).<sup>33,34</sup> The 2-h heating process accelerated molecule

movement, which increased the likelihood of drugs interacting with hydrophobic blocks and getting loaded into the hydrophobic core of MCs.

### 2.3 | Characterization of the drug loaded MCs

The amount of drug loaded inside the micellar formulation could be altered by using different polymer/drug ratios (w/w). For all drug candidates (LE, PA, and DEX), various drug concentrations, including 0.25, 0.5, 1, and 2 (mg/mL), were combined with a fixed concentration (10 mg/mL) of polymers to form drug loaded MCs. The final concentration of drug loaded in 1 mL of MC solution was measured using High Performance Liquid Chromatography (HPLC). As shown in

Figure 3A, with an increase in initially applied drug concentration in the formulation from 0.25 mg/mL to 2 mg/mL, the final concentration of drug loaded inside MCs increased from  $55.7 \pm 10.0$   $\mu\text{g/mL}$  to  $589.2 \pm 75.5$   $\mu\text{g/mL}$  for LE, from  $171.7 \pm 4.2$   $\mu\text{g/mL}$  to  $1154.0 \pm 108.6$   $\mu\text{g/mL}$  for PA, and from  $235.9 \pm 5.0$   $\mu\text{g/mL}$  to  $956.7 \pm 150.3$   $\mu\text{g/mL}$  for DEX. No significant difference in encapsulation efficiency (EE) % of LE and PA with various polymer/drug ratios was detected, while EE % for DEX decreased from  $92.5 \pm 1.7\%$  to  $47.8 \pm 7.5\%$  by increasing the concentration of DEX from 0.5 mg/mL to 2 mg/mL, respectively (Figure 3B). Based on the results of loaded drug concentrations ( $\mu\text{g/mL}$ ) and EE %, 10:1 polymer/drug ratio was selected for further characterization steps including size, PDI and surface charge of drug loaded MCs.

The hydrodynamic sizes of drug loaded MCs were measured by DLS analysis. The average sizes of the LE, PA and DEX loaded MCs were measured to be  $117.30 \pm 0.30$  nm,  $111.40 \pm 0.94$  nm and  $84.30 \pm 0.34$  nm, respectively (Figure 3C). An increase in the sizes of LE and PA drug-loaded MCs was observed compared to the unloaded MCs ( $109.0 \pm 9.16$  nm). In addition, a correlation between decreased size of drug loaded MCs with increased number of H-bond donor groups on the drug molecules was observed. DEX loaded MCs had the smallest size among the three drugs due to the most H-bonding interactions (H-bond donors = 3) between the hydroxyl groups on DEX and the ester oxygen of the hydrophobic MC core, which explained the decreased size of DEX loaded MCs as compared to the unloaded MCs.<sup>33</sup> PDI values for three drug-loaded MCs were  $0.02 \pm 0.01$  (LE),  $0.02 \pm 0.01$  (PA) and  $0.03 \pm 0.02$  (DEX), confirming desired homogeneity and monodisperse of the MC formulations (Figure 3D). The drug loaded MCs had net neutral surface charge density of  $-0.24 \pm 0.40$  mV for LE,  $-0.59 \pm 0.31$  for PA,  $-0.27 \pm 0.51$  for DEX (Figure 3E). Regarding EE and drug loading efficiency (LC), LE showed EE of  $25.5 \pm 2.8\%$  and LC of  $2.5 \pm 0.3\%$  at 10:1 polymer/drug ratio (Figure 3F,G). PA and DEX loaded MCs showed higher EE values of  $57.8 \pm 2.1\%$  and  $74.6 \pm 6.0\%$ , respectively and higher LC values of  $5.5 \pm 0.2\%$  and  $6.9 \pm 0.5\%$ , respectively. These results were in agreement with the hypothesis that in addition to hydrophobic interactions at the core of the MCs, higher number of H-bond donors on the drug molecules supported more H-bonding interactions with hydrophobic core of MCs, which consequently led to higher EE, LC, and smaller MC size.<sup>34</sup>

## 2.4 | *In vitro* release of drugs from the engineered MCs

One important aspect of this study was to achieve a sustained release of drugs on ocular surfaces in order to reduce the eyedrop instillation frequency and improve patient compliance. To this end, *in vitro* release of LE, PA, and DEX from MCs was assessed via a dialysis method under sink conditions.<sup>32</sup> Since LE, PA, and DEX had extremely low aqueous solubility, it was difficult to maintain the molecular dispersion using Dulbecco's phosphate buffered saline (DPBS) alone. A large amount of release media was required to keep the drugs

solubilized, but the drug concentration might be too low to be detectable by HPLC. Therefore, 2% Triton X-100 was added to DPBS buffer as a surfactant to better solubilize the released drug molecules.<sup>32</sup> Previous studies have confirmed that the addition of nonionic surfactants did not induce MC destabilization and did not form mixed MCs due to the different chemical properties of surfactants and copolymers.<sup>32</sup> A change in turbidity of the LE loaded MCs was observed after 5 days of incubation within the release media (Figure 3H). The visible light scattering properties of MCs altered over time as the size and integrity of MCs in the dialysis bag were changed. This was likely due to the hydrolysis of the lactate chains of copolymers, which led to hydrophilization and the swelling of the core of the MCs.<sup>26,30</sup> It was found that LE, PA, and DEX loaded mPEG-b-p(HPMAm-Lac<sub>n</sub>) MCs released their full contents (i.e., drug payload) over the time period of 10 days (Figure 3I). An initial burst release was observed for all three formulations, indicating the presence of residual free drug molecules in the formulation. DEX loaded MCs had the fastest initial release, where 50% of DEX was released after 2 h and 83.1% of DEX was released after 24 h. As compared to DEX, PA loaded MCs showed a slower release rate of 39.4% of PA release after 2 h and 57.3% after 24 h. LE loaded MCs showed the slowest release profile, where 24.2% of LE was released after 2 h and 53.1% after 24 h. The desired administration of topical corticosteroids is an initial burst release combined with gradual and slow release over time. Among all the release profiles, LE loaded MCs showed the desired release profile for ocular drug delivery as compared to other drug loaded MCs. In addition, from pharmacology point of view, LE stands out from PA and DEX molecules because it features an ester at the carbon 20 (C-20) position instead of a ketone.<sup>18</sup> The C-20 ester allows LE to be metabolized into inactive metabolites after exerting therapeutic effects, thereby avoiding adverse effects associated with intraocular pressure (IOP) relative to ketone-based corticosteroids.<sup>35</sup> Therefore, we chose LE encapsulated MCs to be incorporated into the ocular adhesive hydrogel patch and further investigated its properties.

## 2.5 | Fabrication and characterization of unloaded and MCs loaded GelPatch

Our ocular drug delivery platform, GelPatch, is a composite adhesive hydrogel composed of gelatin methacryloyl (GelMA) and hyaluronic acid-glycidyl methacrylate (HAGM), which is loaded with the MCs containing LE. <sup>1</sup>H NMR analysis was performed to determine the degree of methacrylation (DM) of GelMA and HAGM. Comparing <sup>1</sup>H NMR spectra of gelatin and GelMA, new peaks at  $\delta = 5.62$  and  $5.29$  ppm were corresponding to the two protons of methacrylate double bond (Figure S2). In addition, the decreased integration of lysine peaks at  $\delta = 2.75$  ppm further confirmed the reaction of gelatin with methacrylic anhydride.<sup>33</sup> The DM of GelMA was calculated to be 61% based on the percentage of consumption of lysine peaks (Equation 4). HA was reacted with glycidyl methacrylate to form HAGM. The DM of HAGM was defined as the amount of methacrylate groups per one HA disaccharide repeating unit. The DM of

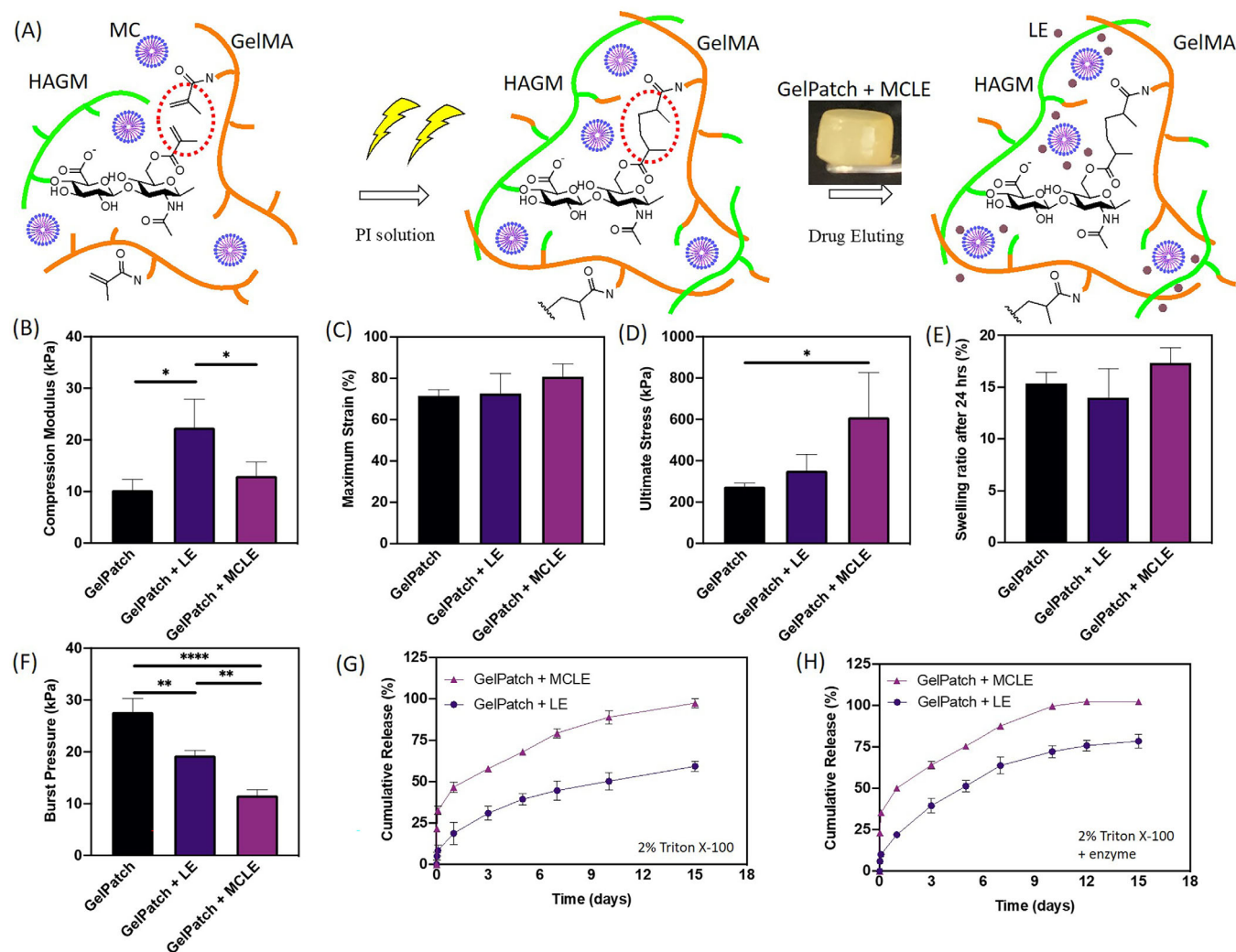


**FIGURE 4** Drug loaded GelPatch formation and characterization. (A) Schematic of photocrosslinking of GelPatch+MCLE prepolymer solution with the photoinitiator (PI) solution (Eosin Y, TEA, and VC) and LE eluting from the crosslinked cylindrical hydrogel. (B) Compression modulus, (C) ultimate strain, (D) ultimate stress, (E) swelling ratio at 37°C in DPBS after 24 h, and (F) burst pressure of GelPatch, GelPatch+LE, and GelPatch+MCLE fabricated using 7% GelMA and 3% HAGM with 4 min photocrosslinking time. (G) *In vitro* release profiles of LE in 2% Triton X-100 releasing medium and (H) *in vitro* release profiles of LE in the presence of 5 µg/mL of collagenase and 5 µg/mL of hyaluronidase in 2% Triton X-100 releasing medium from GelPatch+LE and GelPatch+MCLE at 37°C in 15 days. All hydrogels were polymerized by using 0.5 mM Eosin Y, 1.875% TEA and 1.25% VC in DPBS. Data is represented as means ± SD (\* $p < 0.1$ , \*\* $p < 0.01$ , \*\*\*\* $p < 0.0001$ ).

HAGM was calculated to be 11% based on the ratio of the relative peak integration of methacrylate methyl protons ( $\delta = 1.93$  ppm) to HA's methyl protons ( $\delta = 2.0$  ppm) (Equation 5, Figure S3). The synthesized GelMA (7%(w/v)) and HAGM (3%(w/v)) were then mixed with the photoinitiator (PI) solution, which consisted of Eosin Y initiator, triethanolamine (TEA) and N-vinylcaprolactam (VC) as described in our previous work.<sup>16</sup> The precursor solution of GelPatch had a viscosity of  $23 \pm 2.5$  Pa s. Finally, GelPatch hydrogel was formed by photocrosslinking the mixture under visible light for 4 min.<sup>16</sup> To prepare GelPatch containing LE loaded MCs, named as GelPatch+MCLE, LE loaded MCs were mixed with dissolved GelMA and HAGM in the PI solution before photocrosslinking as illustrated in Figure 4A. In addition, free LE loaded GelPatch, named as GelPatch+LE, was made by mixing free LE with GelPatch prepolymer solution prior

photocrosslinking. No significant differences in viscosity of GelPatch+MCLE and GelPatch+LE compared to the GelPatch precursor solution was detected. Crosslinked hydrogel cylinders were obtained and used to evaluate the mechanical properties and *in vitro* swelling ratio.

The mechanical properties of GelPatch hydrogels with and without MCs were determined through compression tests (Figure 4B–D). The loading of free LE doubled the compression modulus from  $10.30 \pm 2.03$  kPa to  $22.39 \pm 5.52$  kPa as compared to GelPatch, while the incorporation of LE loaded MCs did not significantly change the compression modulus which was measured as  $13.02 \pm 2.67$  kPa (Figure 4B). The increased compression modulus of GelPatch+LE could be due to the presence of aggregated LE particles dispersed as crystalline domains inside the GelPatch hydrogel due to their poor aqueous solubility, whereas for GelPatch+MCLE, there was no

solubility issue, since MCs well solubilized LE before loading into GelPatch. There was no significant difference in the ultimate strain among GelPatch, GelPatch+LE and GelPatch+MCLE (Figure 4C). Furthermore, the ultimate stress of GelPatch increased from  $276.0 \pm 15.52$  kPa to  $610.8 \pm 215.43$  kPa after the addition of LE loaded MCs but did not change after loading free LE (Figure 4D). These results indicated that the dispersion of MCs within the hydrogel matrix can strengthen the resistance to the deformation of the GelPatch hydrogels.

The swelling ratios for different formulations including GelPatch, GelPatch+LE, and GelPatch+MCLE were also evaluated (Figure 4E). GelPatch itself had a swelling ratio of  $15.38 \pm 1.06\%$  in DPBS at  $37^\circ\text{C}$  after 24 h. It was found that the addition of free LE and LE loaded MCs had no significant effect on the swelling ratio of GelPatch, and the values were measured to be  $14.01 \pm 2.81\%$  and  $17.32 \pm 1.52\%$  for GelPatch+LE and GelPatch+MCLE, respectively.

The adhesive properties of the patches were essential since the hydrogels would be applied as drug delivery matrix loaded with solubilized drug molecules that will adhere to the ocular surface and directly deliver anti-inflammatory drugs to the site of inflammation. Therefore, the adhesive properties of GelPatch, GelPatch+LE, and GelPatch+MCLE to the biologic surfaces were evaluated. *In vitro* burst pressure tests were performed based on a modified ASTM standard test (F2392-04) for GelPatch, GelPatch+LE and GelPatch+MCLE. The results showed that the burst pressure of GelPatch decreased from  $27.7 \pm 2.6$  kPa to  $19.35 \pm 0.95$  kPa after the addition of free LE and further decreased to  $11.6 \pm 1.1$  kPa after the incorporation of LE loaded MCs. The adhesion to collagen sheet, which was used as a biological substrate in this test, was due to the various chemical bond formation and physical interactions at the substrate/hydrogel interface. Although the addition of LE loaded MCs changed the intermolecular interactions within GelPatch as well as its surface layer composition, which reduced the interface adhesion, GelPatch+MCLE still maintained an improved adhesive strength of  $11.6 \pm 1.1$  kPa compared to several commercially available surgical sealants such as Eviceal ( $3.2 \pm 1.3$  kPa), CoSEAL ( $1.7 \pm 0.1$  kPa), Duraseal ( $3.6 \pm 0.9$  kPa) and fibrin sealant ( $4.3 \pm 0.7$  kPa).<sup>16,36,37</sup>

## 2.6 | *In vitro* release of LE from GelPatch

*In vitro* release profiles of LE from GelPatch+LE and GelPatch+MCLE were obtained in 2% Triton X-100 in DPBS with and without enzymes. As shown in Figure 4G, 88.9% of LE was released from GelPatch+MCLE in 10 days and 100% was released after 15 days. On the other hand, only 50.2% of LE was released from GelPatch+LE in 10 days and 59.3% was released after 15 days. The slower release of LE from GelPatch+LE could be due the fact that free LE remained in crystalline domains inside GelPatch and its release was entirely based on the swelling of GelPatch and solubilization via diffused Triton X-100 surfactant in the release media. However, for the GelPatch+MCLE, the release of LE can be described due to two continuous processes. LE loaded MCs were able to diffuse out slowly from

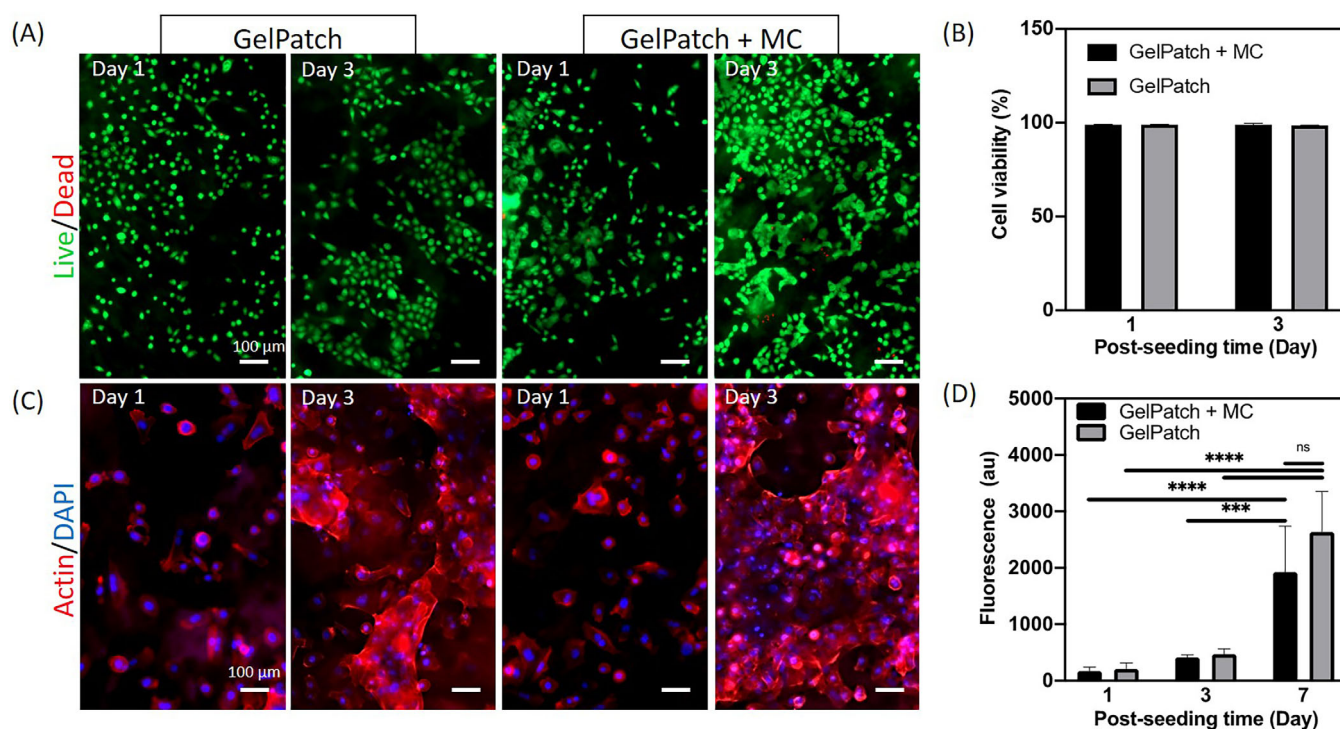
GelPatch and then the hydrolysis of MCs happened in the release media where LE then got released. Simultaneously, the entrapped MCs could be hydrolyzed even slower within GelPatch and later LE was diffused out from GelPatch directly. These two processes explained the slower LE release profile from the GelPatch+MCLE matrix as compared to the LE release profile just from MCs. In order to assess the release profile in the presence of enzymes to mimic the real eye environment, we added  $5 \mu\text{g/mL}$  of collagenase and  $5 \mu\text{g/mL}$  of hyaluronidase in the 2% Triton X-100 release media. As shown in Figure 4H, the overall release of LE in the presence of enzyme solution was faster from both GelPatch+LE and GelPatch+MCLE. It was found that 99.5% of LE was released from GelPatch+MCLE in 10 days and full release was obtained within 12 days. For GelPatch+LE, 72.2% of LE was released in 10 days and 78.5% after 15 days. The increased release rate in the presence of enzyme was due to the faster enzymatic degradation of GelPatch, which resulted in decreasing polymer network density and increasing patch pore sizes. Therefore, MCs diffused out faster from GelPatch leading to a faster release of LE observed in Figure 4H. These release profile data supported the study objective of the sustained release of anti-inflammatory LE to treat ocular injuries.

## 2.7 | *In vitro* biocompatibility of drug loaded GelPatch

To evaluate the biocompatibility of GelPatch loaded MC, the viability and metabolic activity of the seeded hTCEpi cells on the crosslinked samples were investigated through Live/Dead assay and PrestoBlue assay at days 1, 3, and 7. The micrographs of stained cells based on Live/Dead assay at day 1 and day 3 showed high viability of cells (>90%) seeded on GelPatch with and without MCs at the early stage of their culture (Figure 5A,B). In addition, the morphology of the cultured cells on the hydrogels was evaluated by fluorescent F-actin staining of the cytoskeleton of cells on day 1 and day 3. The assembly of F-actin cytoskeleton of cells in fluorescent micrographs showed that the cells adhered and spread on the surfaces of both GelPatch and GelPatch with MCs, indicating the *in vitro* biocompatibility of the samples for cell adherence and growth (Figure 5C). The metabolic activity of cultured hTCEpi cells on samples through PrestoBlue assay showed a consistent increase over 7 days for both GelPatch and GelPatch containing MCs (Figure 5D).

## 2.8 | *In vivo* biocompatibility and biodegradation of GelPatch using a rat subcutaneous model

Lastly, subcutaneous implantations of GelPatch and GelPatch+MC in rats were performed to investigate their *in vivo* biocompatibility and biodegradation. Following explanation of the samples, they were stained with Hematoxylin and Eosin (H&E). The H&E stained images showed a small amount of cell infiltration in both GelPatch and GelPatch+MC (Figure 6A). Based on Masson's Trichrome (MT) staining in



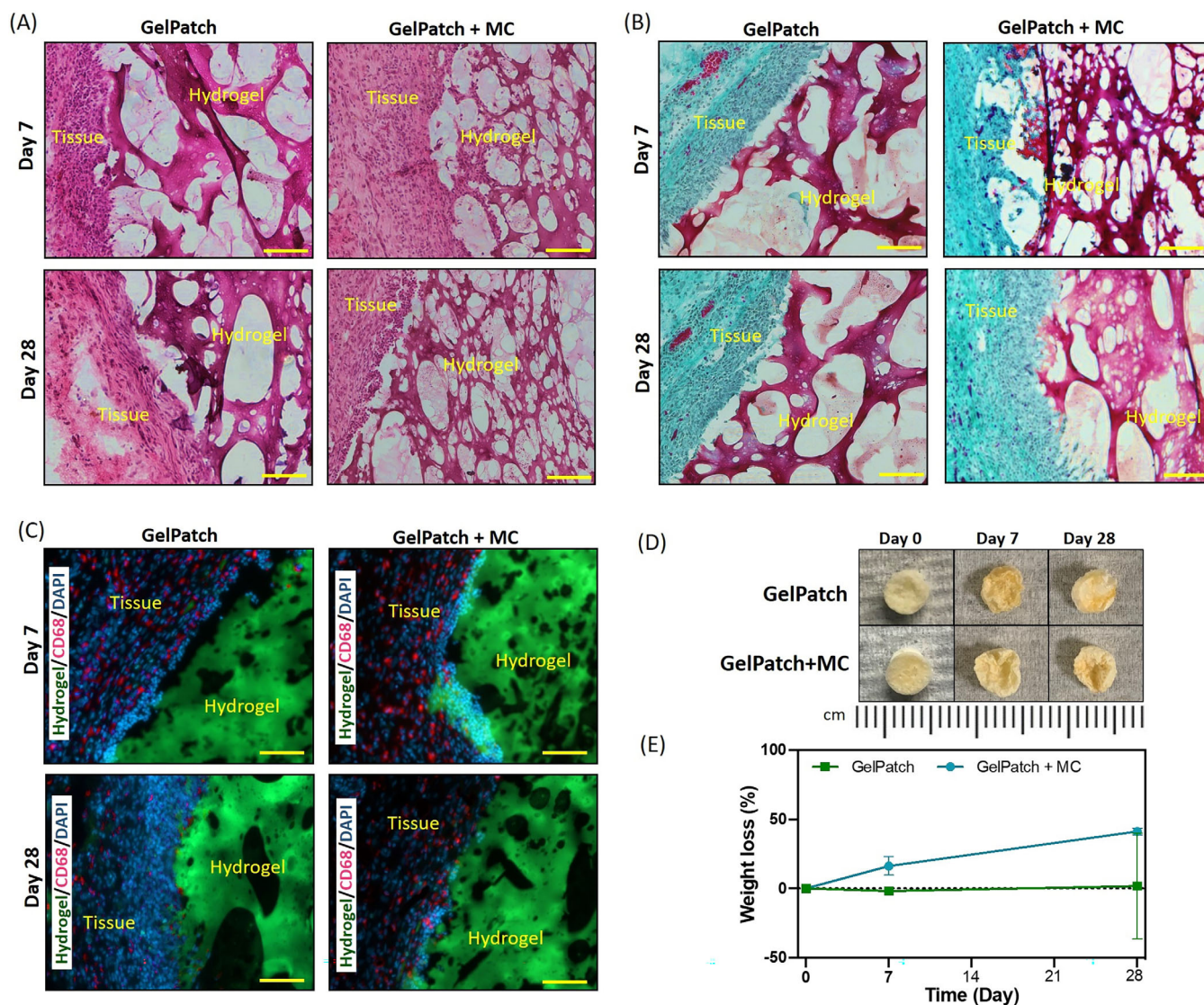
**FIGURE 5** *In vitro* biocompatibility of GelPatch and GelPatch containing MCs. (A) Representative LIVE/DEAD images from hTCEpi cells seeded on hydrogels on day 1 and 3 (scale bar, 100  $\mu\text{m}$ ). (B) Quantification of cell viability on GelPatch and GelPatch+MC after 1 and 3 days of culture. (C) Representative Actin/DAPI images from hTCEpi cells seeded on hydrogels on day 1 and 3 (scale bar, 100  $\mu\text{m}$ ). (D) Quantification of metabolic activity of hTCEpi cells seeded on GelPatch and GelPatch+MC after 1, 3, and 7 days. Data is represented as means  $\pm$  SD (\*\*\* $p$  < 0.001, \*\*\*\* $p$  < 0.0001,  $n \geq 3$ ).

Figure 6B, no significant fibrosis was detected in both hydrogels. In addition, immunofluorescence analysis of subcutaneously implanted hydrogels demonstrated the presence of macrophages (CD68) at day 7, but they significantly reduced at day 28 (Figure 6C). The results of *in vivo* biodegradation study showed that there was no statistically significant change after 28 days, as demonstrated by visual inspection (Figure 6D) and measurements in the weight loss of the samples (Figure 6E). The large error bar seen in the percentage of weight loss of GelPatch samples (Figure 6E) might be due to the variance of entrapment of adjacent tissues in the hydrogel samples, as the presence of red color shown in the images of the lyophilized hydrogels post-implantation (Figure 6D). These results suggested that GelPatch encapsulated with MCs was biocompatible and was able to retain in its stability after 28 days, which would allow sustained full release of drugs before degradation of the GelPatch.

### 3 | DISCUSSION

In this study, we developed an anti-inflammatory drug eluting adhesive patch for sustained release of anti-inflammatory therapeutics after ocular injuries. As drug carriers, mPEG-b-p(HPMAm-Lac<sub>n</sub>) MCs successfully solubilized hydrophobic corticosteroids, through H-bonding and hydrophobic interactions. They were loaded inside the hydrogel and provided sustained release of the

drugs as demonstrated in the *in vitro* release studies. In addition, photocrosslinkable adhesive GelPatch showed appropriate mechanical strength, adhesion, and swelling properties as an ocular drug delivery platform. The incorporation of LE loaded MCs in GelPatch had no significant effect on the mechanical properties or the swelling properties of the hydrogel. Despite a small decrease in burst pressure, GelPatch+MCLE still maintained an improved adhesive strength compared to several commercially available surgical sealants and was able to achieve a sustained full release of LE in 15 days without enzymes and in 12 days in the presence of collagenase and hyaluronidase. Moreover, *in vitro* cell studies showed that MC loaded GelPatch were biocompatibility and supported cellular adhesion, proliferation, and growth. *In vivo* subcutaneous studies further proved the biocompatibility of the engineered drug eluting adhesive patch. The developed non-invasive, adhesive, and biocompatible GelPatch containing LE loaded MCs have the potential to provide several advantages in the future over the conventional drug delivery methods such as improved patient compliance, site-targeted delivery. The MC loaded GelPatch system showed good capacity to incorporate other hydrophobic therapeutics. It has the potential to become a promising ocular drug delivery platform for treatment of different ocular anterior segment diseases and injuries. It is important to note that in the current reported *in vitro* drug release profiles for MC loaded GelPatch were based on using a synthetic surfactant in the release media. Further



**FIGURE 6** *In vivo* biocompatibility and biodegradability of GelPatch and GelPatch+MC using a rat subcutaneous model. (A) Hematoxylin and Eosin (H&E) stained, (B) Masson's Trichrome (MT) stained, and (C) immunofluorescence (IF) stained images of GelPatch and GelPatch+MC samples (hydrogels with the surrounding tissue) after 7 and 28 days of implantation (scale bar, 100  $\mu$ m). (D) Representative images of GelPatch and GelPatch+MC hydrogels before implantation (day 0), and on days 7 and 28 post-implantation. (E) *In vivo* biodegradation of hydrogels on days 7 and 28 post-implantation. Data is represented as means  $\pm$  SD.

investigations on the drug release profile using appropriate *ex vivo* and *in vivo* models is necessary to better evaluate the efficacy of the engineered MC loaded GelPatches. In addition, further optimizations are required to increase the drug loading efficiency in the micellar formulation to achieve the desired therapeutic concentrations of released drug molecules at the ocular anterior segment.

## 4 | MATERIALS AND METHODS

### 4.1 | Materials

4,4-Azobis(4-cyanopentanoic acid) (ABCPA), poly(ethylene glycol) methyl ether (Mw 5000 g/mol) (mPEG), N,N'-Dicyclohexylcarbodiimide

(DCC), 4-dimethylaminopyridine (DMAP), and p-toluenesulfonic acid, L-lactide, N-(2-hydroxypropyl)methacrylamide (HPMAm), Tin(II) 2-ethylhexanoate (SnOct<sub>2</sub>), and 4-methoxyphenol were purchased from Sigma-Aldrich. All solvents: tetrahydrofuran (THF), dichloromethane (DCM), dimethylformamide (DMF), acetonitrile (ACN), and acetone were provided by Sigma-Aldrich or Fisher Chemical. Nuclear magnetic resonance (NMR) solvents: chloroform-d (CDCl<sub>3</sub>), deuterated dimethyl sulfoxide (DMSO-d<sub>6</sub>) and deuterium oxide (D<sub>2</sub>O) were purchased from Cambridge Isotope Laboratories, Inc. Gelatin from porcine skin (Gel strength 300, type A), methacrylic anhydride, hyaluronic acid sodium salt from Streptococcus equi, glycidyl methacrylate (GM), Eosin Y disodium salt, triethanolamine (TEA) and N-vinylcaprolactam (VC), Triton X-100 were all purchased from Sigma-Aldrich.

## 4.2 | Synthesis of micelles

### 4.2.1 | Synthesis of macroinitiator mPEG<sub>2</sub>-ABCPA

Macroinitiators mPEG<sub>2</sub>-ABCPA were synthesized through an esterification of mPEG and ABCPA using DCC as a coupling reagent and 4-(dimethylamino)pyridinium 4-toluenesulfonate (DPTS, which was made by 1:1 molar ratio of DMAP and p-toluenesulfonic acid in THF) as a catalyst, as described in Bagheri et al.<sup>38</sup> In brief, 1 equiv. of ABCPA (0.280 g), 2 equiv. of PEG (10 g), and 0.3 equiv. of DPTS (36.7 mg of DMAP and 57.3 mg of p-toluenesulfonic acid each separately dissolved in 1 mL of THF) were dissolved in 50 mL of dry DCM with stirring on ice bath. Vacuum and nitrogen alternating cycles were repeated three times. Next, 3 equiv. of DCC (0.619 g) were dissolved in 50 mL of dry DCM and dropwise added to PEG solution under nitrogen atmosphere. After the addition of DCC, the ice bath was removed allowing the mixture to react at room temperature. After 16 h, the reaction mixture was filtered to remove 1,3-dicyclohexyl urea salts and was dried under vacuum to remove solvents. Then, the remaining product was redissolved in water, stirred for 2 h, and dialyzed against water for 72 h at 4°C. The final white product was obtained by freeze-drying and was analyzed by Gel Permeation Chromatography (GPC) in DMF and Proton Nuclear Magnetic Resonance (<sup>1</sup>H NMR) spectroscopy in CDCl<sub>3</sub>.

### 4.2.2 | Synthesis of monomer HPMAm-Lac<sub>n</sub>

A mixture of 1 equiv. of L-lactide (1 g), 1 equiv. of HPMAm (0.993 g), 0.01 equiv. of SnOct<sub>2</sub> (28.1 mg, 1 mol% relative to HPMAm), and 0.001 equiv. of 4-methoxyphenol (0.86 mg, 0.1 mol% relative to HPMAm) were added in a round bottom flask.<sup>26</sup> Vacuum and nitrogen alternating cycles were repeated three times to remove air. Then, the mixture was heated to 130°C with stirring for 1 h and allowed to cool to room temperature.

The purification was performed through a silica column chromatography. The reaction mixture was first dissolved in small amount of ethyl acetate (EtOAc) and dry-loaded on a silica column. A 90% EtOAc/Hexane solvent system was used to run the column entirely. Thin Layer Chromatography (TLC) was used to analyze the separation. The fractions containing HPMAm-Lac<sub>n</sub> were collected, and after solvent evaporation, the identity of obtained fractions was established by <sup>1</sup>H-NMR in CDCl<sub>3</sub>. <sup>1</sup>H NMR for monomer HPMAm-Lac<sub>n</sub> (CDCl<sub>3</sub>, 400 MHz): Chemical shift (δ, ppm) = 6.32–6.04 (b, 1H, H<sub>3</sub>), 5.71 (s, 1H, H<sub>1</sub>), 5.35 (s, 1H, H<sub>1</sub>'), 5.2–5.0 (m, H<sub>5</sub>, H<sub>8</sub>), 4.36 (q, 1H, H<sub>9</sub>), 3.62 (m, 1H, H<sub>4</sub>), 3.37 (m, 1H, H<sub>4</sub>'), 1.96 (s, 3H, H<sub>2</sub>), 1.50 (d, 6H, H<sub>7</sub>, H<sub>10</sub>), 1.27 (d, 3H, H<sub>6</sub>).

### 4.2.3 | Synthesis of copolymer mPEG-b-p(HPMAm-Lac<sub>n</sub>)

The mPEG-b-p(HPMAm-Lac<sub>n</sub>) was synthesized by radical polymerization using mPEG<sub>2</sub>-ABCPA as macroinitiator and HPMAm-Lac<sub>n</sub> as

monomer, as described previously.<sup>26,29</sup> Monomer to macroinitiator feed ratio was 150:1. A mixture of HPMAm-Lac<sub>n</sub> and mPEG<sub>2</sub>-ABCPA were dissolved in dry ACN. The concentration of macroinitiator plus monomer was 300 mg/mL in ACN. The resulting solution was degassed by freeze-pump-thaw method and then heated to 70°C with stirring for 24 h. After 24 h, the reaction was cooled to room temperature and diluted in a small amount of ACN (~2 mL). The product in the solution was precipitated by dropwise addition to an excess of cold diethyl ether (~45 mL) in a 50 mL vial. After centrifugation at 3000 rpm for 15 min, a white pellet was obtained. Diethyl ether wash followed by centrifugation was repeated three times. Followed by dissolution in water, product solution was dialyzed (MWCO 12–14 kDa) against water and finally recovered by freeze drying. The final product was analyzed by GPC and <sup>1</sup>H-NMR. <sup>1</sup>H NMR for copolymer mPEG-b-p(HPMAm-Lac<sub>n</sub>) (CDCl<sub>3</sub>, 400 MHz): δ = 6.6 (b, H<sub>1</sub>), 5.3–4.8 (b, H<sub>3</sub>, H<sub>4</sub>), 4.39 (b, H<sub>5</sub>), 3.64 (b, PEG CH<sub>2</sub>-CH<sub>2</sub>), 3.3–2.7 (b, H<sub>2</sub>), 2.4–0.4 (the rest of the protons).

### 4.2.4 | Preparation of unloaded and drug loaded MCs

Drug loaded MCs were formed by self-assembly via a solvent evaporation method as described before with some modifications.<sup>32</sup> Briefly, 10 mg of copolymers mPEG-b-p(HPMAm-Lac<sub>n</sub>) were dissolved in 1 mL of acetone. Various amounts of drugs (0.25, 0.5, 1, and 2 mg) were then added to the copolymer solution and vortexed until fully mixed. Next, polymer/drug cocktail solution was quickly added to 1 mL of ammonium acetate buffer (120 mM, pH 5) with stirring. The mixture was stirred at room temperature for 30 min and then heated to 45°C. After 2 h, the mixture was slowly cooled down to room temperature and stirred overnight. The next day, the MC solution was centrifuged at 4000 rpm at 22°C for 10 min to remove unencapsulated drugs. LE, PA, and DEX were three drugs of interest. 30 mg/mL of drug stock solutions were prepared in DMSO. Unloaded MCs were prepared with the same procedure without the addition of drugs.

## 4.3 | Fabrication of GelPatch

### 4.3.1 | Synthesis of GelMA

GelMA was synthesized as described previously.<sup>16,17</sup> In brief, 10% (w/v) gelatin from porcine skin (Bloom 300, type A, Sigma) was dissolved in DPBS and 8% (v/v) methacrylic anhydride was added dropwise at 55°C. The mixture was allowed to react for 3.5 h under continuous stirring. The reaction was stopped by two times dilution in DPBS and was dialyzed against water at 50°C for 5 days. Finally, the resulting solution was frozen at –80°C for 24 h and freeze-dried for 5 days to yield GelMA.

### 4.3.2 | Synthesis of HAGM

Hyaluronic acid (HA) was modified with Glycidyl methacrylate (GM) to form HAGM using a previously described protocol with some modifications.<sup>17,39</sup> In brief, 1% (w/v) of HA (1.6 MDa, Sigma) was dissolved in 200 mL deionized water for 12 h under continuous stirring. After it fully dissolved, 8 mL triethylamine, 8 mL GM, and 4 g of tetrabutyl ammonium bromide (TBAB) were added in order separately and thoroughly mixed for 1 h before the next addition. Following complete dissolution, the reaction was allowed to continue overnight (16 h, 22°C) and was finally completed by incubation at 60°C for 1 h. After cooling to room temperature, the solution was then precipitated in 20 times excess volume of acetone (4 L) as white solid fibers. The precipitate was then dissolved in water, dialyzed for 2 days and lyophilized.

### 4.3.3 | Preparation of unloaded and loaded GelPatch

GelPatch prepolymer was prepared by mixing GelMA and HAGM with a photoinitiator (PI) solution. The PI solution was prepared by dissolving 0.5 mM Eosin Y disodium salt, 1.86% (w/v) TEA and 1.25% (w/v) VC in phosphate buffered saline (PBS). 1 N hydrochloric acid was used to adjust the pH of PI solution to 8. Then, 7% (w/v) GelMA and 3% (w/v) HAGM were thoroughly mixed in PI solution and incubated at 50°C overnight. After complete dissolution, the final GelPatch prepolymer solutions were crosslinked for 4 min with visible light (450–550 nm) by using an LS1000 Focal Seal Xenon Light Source (100 mW/cm<sup>2</sup>, Genzyme). GelPatch containing free LE (GelPatch+LE) and GelPatch containing LE loaded MCs (GelPatch+MCLE) were prepared with an additional step of physically mixing LE powder or MC solutions with dissolved GelMA and HAGM in PI solution before crosslinking.

## 4.4 | Characterization

### 4.4.1 | <sup>1</sup>H NMR spectroscopy and formulas

#### <sup>1</sup>H NMR analysis of macroinitiator, monomer and copolymer

The <sup>1</sup>H NMR spectra of macroinitiator, monomer and copolymer were obtained in CDCl<sub>3</sub> using a Bruker AV 400 MHz NMR Spectrometer (2 s delay and 64 scans). The chemical shift of CDCl<sub>3</sub> at 7.26 ppm was used as reference line. The average molecular weight of HPMAm-Lac<sub>n</sub> (Mw<sub>ave,HPMAm-Lac<sub>n</sub></sub>), the number of HPMAm-Lac<sub>n</sub> repeating units (m) and the average molecular weight of mPEG-b-p (HPMAm-Lac<sub>n</sub>) (Mn) were determined by <sup>1</sup>H NMR, using the following equations (1–5):

$$Mw_{ave,HPMAm-Lac_n} = \%Lac_2 \times 287.31 + \%Lac_3 \times 359.38 + \%Lac_4 \times 431.44 \quad (1)$$

$$m = \frac{I_{CO-CH(CH_3)-OH}}{I_{PEG_{5k}}/454} \quad (2)$$

$$Mn = Mw_{PEG_{5k}} + m \times Mw_{ave,HPMAm-Lac_n} \quad (3)$$

where  $I_{CO-CH(CH_3)-OH}$  is the value of the integration of the methine proton next to the hydroxyl group (Figure 1D, H<sub>5</sub>, δ = 4.39 ppm).  $I_{PEG_{5k}}/454$  is the ratio of the integration of PEG<sub>5k</sub> proton to the average number of protons per PEG<sub>5k</sub> chain.

#### <sup>1</sup>H NMR analysis of GelMA and HAGM

The gelatin and GelMA were dissolved in DMSO-d<sub>6</sub> and HAGM was dissolved in D<sub>2</sub>O at a concentration of 10 mg/mL and at a temperature of 50°C. The <sup>1</sup>H NMR spectra were recorded with a Bruker AV 400 MHz NMR Spectrometer (10 s delay and 64 scans). The degree of methacrylation (DM) of GelMA was defined as the ratio of methacrylate groups to the free amine groups in gelatin prior to the reaction.<sup>15</sup> The vinyl protons on methacrylamide grafts gave rise to two peaks at δ = 5.62 and 5.29 ppm. The peak areas of methylene protons of lysine groups (δ = 2.75 ppm) in the spectra of gelatin and GelMA were integrated separately. The DM of GelMA was calculated from the following equation.

$$DM(\%) = 1 - \frac{I_{lysine}(GelMA)}{I_{lysine}(Gelatin)} \times 100\% \quad (4)$$

The DM of HAGM was defined as the amount of methacryloyl groups per one HA disaccharide repeating unit.<sup>39</sup> The two vinyl protons on methacrylate groups had chemical shifts of 6.16 and 5.16 ppm. The DM was calculated from the ratio of the relative peak integrations of the methyl protons of methacrylate groups (δ = 1.93 ppm) to the methyl protons of amide groups (δ = 2 ppm) on HA.

$$DM(\%) = \frac{I_{H_3}(\text{methyl Hs on GM})/3}{I_{H_4}(\text{methyl Hs on HA})/3} \times 100\% \quad (5)$$

### 4.4.2 | Gel permeation chromatography (GPC)

Analysis of the mPEG<sub>2</sub>-ABCPA macroinitiator and mPEG-b-p (HPMAm-Lac<sub>n</sub>) copolymer was performed using a Waters System (Waters Associates Inc., Milford, MA) with refractive index (RI) using two serial PLgel 5 μm MIXED-D columns (Polymer Laboratories) and THF as eluent. The flow rate was 0.7 mL/min (45 min run time) and the temperature was 25°C. The molecular weights of the synthesized polymers were determined by GPC analysis using RI detector and standards to calculate the number average molecular weight (Mn), the weight average molecular weight (Mw), and polydispersity index (PDI; (Mw/Mn)).

#### 4.4.3 | Dynamic light scattering (DLS)

Freshly prepared micellar dispersions were diluted 25 times with 10 mM HEPES, pH 7.0 (final concentration 400  $\mu\text{g}/\text{mL}$ ) and their sizes were analyzed with a Malvern Zetasizer Nano dynamic light scattering. Standard operating procedure parameters: 10 runs, 10 s/run, three measurements, no delay between measurements, 25°C with 120 s equilibration time. Collection parameters: S26 lower limit = 0.6, upper limit = 1000, resolution = high, number of size classes = 70, lower size limit = 0.4, upper size limit = 1000, lower threshold = 0.05, upper threshold = 0.01. Data is representative of three replicate measurements.

#### 4.4.4 | Zeta potential

Zeta potential of the MCs was determined using a Malvern Zetasizer Nano-Z (Malvern Instruments, Malvern, UK) with universal ZEN 1002 “dip” cells and DTS (Nano) software (version 4.20) at 25°C. Zeta potential measurements were performed in 10 mM HEPES at pH 7.4 at a final polymer concentration of 400  $\mu\text{g}/\text{mL}$ .

#### 4.4.5 | Transmission electron microscopy (TEM)

The sample preparation for cryo-TEM was performed in a temperature and humidity-controlled chamber using a fully automated vitrification robot (FEI Co., Hillsboro, OR). A thin aqueous film of MC solution was formed on a Quantifoil R 2/2 grid (Quantifoil Micro Tools GmbH, Jena, Germany) at 22°C and at 100% relative humidity. This thin film was rapidly vitrified by shooting the grid into liquid ethane. The grids with the vitrified thin films were transferred into the microscope chamber using a Gatan 626 cryo-transfer/cryo-holder system (Gatan, Inc., Pleasanton, CA). Micrographs were taken using a CM-12 transmission microscope (Philips, Eindhoven, The Netherlands) operating at 120 kV, with the specimen at  $-170^\circ\text{C}$  and using low-dose imaging conditions.

#### 4.4.6 | Rheological measurement

Oscillatory rheology measurements of hydrogel precursor solution were carried with an Anton Paar (MCR 302) by utilizing a cone plate (radius 8 mm, cone angle  $2^\circ$ ). A solvent trap was used to minimize water evaporation during the measurement. Rheology measurement was performed at 25°C. Amplitude sweeps, with shear rates ( $\dot{\gamma}$ ) ranging from 0.1 to 100  $\text{s}^{-1}$  at 25°C under flow conditions, were performed at a frequency of  $\omega = 1 \text{ Hz/s}$ .

#### 4.4.7 | Determination of encapsulation efficiency and loading capacity

The amount of loaded drug molecules (LE, PA, and DEX) in the polymeric MCs was determined by using High Performance Liquid

Chromatography (HPLC). Taking LE as an example, after centrifugation of the MC solution, the unencapsulated LE pellet was redissolved in 1 mL of ACN. The concentration of this solution was measured by HPLC using a 70%–90% ACN/water gradient solvent system at 242 nm (60%–80% gradient at 243 nm for PA and 50%–80% gradient at 239 nm for DEX). LE dissolved in ACN (concentration from 0.1 mg/mL to 1 mg/mL) was used for calibration. The encapsulation efficiency (EE) and loading capacity (LC) (Equations 6, 7) were calculated as follows:

$$\text{EE}\% = 1 - \frac{\text{amount of unloaded drugs}}{\text{amount of drugs used for loading}} \times 100\% \quad (6)$$

$$\text{LC}\% = 1 - \frac{\text{amount of unloaded drugs}}{\text{amount of copolymer used for loading}} \times 100\% \quad (7)$$

#### 4.4.8 | Mechanical characterization

For the unconfined compression test, 75  $\mu\text{L}$  of hydrogel precursor solution was pipetted into a polydimethylsiloxane (PDMS) cylindrical mold (diameter: 6 mm; height: 2.5 mm). The resulting solution was photocrosslinked via exposure to visible light for 4 min. After photocrosslinking, the dimensions of the hydrogels were measured using a digital caliper. The compression tests were conducted using an Instron 5943 mechanical tester. The crosslinked hydrogel cylinders were placed between the compression plates and compressed at a rate of 1 mm/min until failure. The slope of the stress–strain curves was obtained and reported as the compression modulus<sup>40,41</sup> ( $N = 3$ ).

#### 4.4.9 | *In vitro* burst pressure test

Burst pressure resistance (i.e., Adhesion strength) of the composite hydrogel formulations was measured by using the ASTM F2392-04 standard according to a previously reported method.<sup>16,42</sup> Briefly, collagen sheet made out of porcine intestine ( $4 \times 4 \text{ cm}$ ) was placed in between two stainless steel annuli from a custom-built burst pressure device, which consists of a metallic base holder, pressure meter, syringe pressure setup, and data collector. A hole (2 mm diameter) was created through the sheet and was sealed (photocrosslinked) by applying 30  $\mu\text{L}$  of hydrogel precursor solution. Next, the airflow was applied into the system, and the maximum burst pressure was recorded until detachment from the collagen sheet or hydrogel rupture. The burst pressure resistant was measured using a pressure sensor connected to a computer. Three replicates were performed for each hydrogel sample.

#### 4.4.10 | Measurement of swelling ratio

Hydrogel samples were prepared as described in previous section. The weight of each hydrogel sample ( $N = 3$ ) was measured following photocrosslinking and after 24 h in DPBS at 37°C. The swelling ratio

was then calculated according to the equation below, where  $W_0$  is the weight of the sample just after photocrosslinking and  $W_1$  is the final weight of the sample after 24 h incubation.

$$\text{Swelling ratio (\%)} = \frac{W_1 - W_0}{W_0} \times 100 \quad (8)$$

#### 4.4.11 | *In vitro* release profile from MCs and GelPatch loaded MCs

The release profiles of LE, PA, and DEX from the polymeric MCs were examined by a dialysis method.<sup>32</sup> Taking LE as an example, 1 mL of LE loaded MC solution was pipetted into a dialysis bag (MWCO 12–14 kDa). The releasing medium was prepared with a solution of 2% Triton X-100 in DPBS. The dialysis bag was immersed in 10 mL of the releasing medium with stirring at 300 rpm at 37°C. Samples (5 mL) of the receiving medium were drawn periodically and 5 mL of fresh releasing medium were added back to keep the volume constant. The concentration of LE in the different samples was measured using HPLC method mentioned in previous section. Calibration was done using LE (concentration from 0.005 mg/mL to 0.1 mg/mL) in 2% Triton X-100 in DPBS.

*In vitro* release profiles of LE from GelPatch+MCLE and GelPatch+LE were measured using the same releasing medium. A 250  $\mu$ L of GelPatch+MCLE precursor solution was pipetted into cylindrical mold and photocrosslinked for 4 min. The gel cylinder was then immersed in 10 mL of releasing medium (2% Triton X-100 in DPBS) in an incubator shaker at 75 rpm at 37°C. Samples (5 mL) of the receiving medium were drawn periodically and fresh releasing medium were added back to keep the volume constant. The concentration of LE in the different samples ( $N = 3$ ) was measured by HPLC. Additionally, *in vitro* release profile in the presence of enzymes were studied by adding 5  $\mu$ g/mL of collagenase and 5  $\mu$ g/mL of hyaluronidase on top of 2% Triton X-100 releasing medium with all other procedures remaining the same.

#### 4.4.12 | *In vitro* biocompatibility of GelPatch and MC loaded GelPatch (GelPatch+MC)

hTCEpi cells were cultured at 37°C and 5% CO<sub>2</sub> in KBM™ basal media (00192151) supplemented with KGM-Gold™ Keratinocyte Single-Quots™ Kit (00192152). The cells were seeded on the surface of the hydrogel scaffolds as defined elsewhere.<sup>43</sup> Briefly, 10  $\mu$ L of GelPatch precursor solutions were spread and photocrosslinked on a 3-(trimethoxysilyl) propyl methacrylate (TMSPMA)-coated glass slide, providing 1  $\times$  1 cm<sup>2</sup> surface areas of hydrogels. Samples ( $N \geq 3$ ) were placed in 24 well-plate and hTCEpi cells were seeded on the hydrogel surface (10<sup>5</sup> cells per sample). After incubation of the seeded samples in a humid incubator with 5% CO<sub>2</sub> for 20 min at 37°C, 400  $\mu$ L of media was added to each well and incubated. The media was replaced with fresh media every other day.

The viability of cultured cells on the gel scaffolds at day 1 and day 3 was evaluated using a Live/Dead™ Viability/Cytotoxicity Kit

(Invitrogen) as stated by the manufacturer's instructions. Briefly, a solution of calcein AM at 0.5  $\mu$ L/mL (green color, viable cells) and ethidium homodimer at 2  $\mu$ L/mL (red color, nonviable cells) in DPBS was used to stain the cells. After 15 min of incubation, samples were washed with DPBS, and cells were imaged using a fluorescence optical microscope (Primovert, Zeiss). The collected images were analyzed using the ImageJ software to quantify the cell viability (%) by dividing the number of live cells by the total number of live and dead cells.

Proliferation and metabolic activity of cells were determined using a PrestoBlue assay (Invitrogen) at day 1, 3, and 7 after culture according to the manufacturer's instructions. Briefly, seeded samples were incubated with a media solution containing 10% PrestoBlue reagent for 45 min with 5% CO<sub>2</sub> at 37°C. The Fluorescence intensity of the solution was determined using a plate reader (BioTek) at 540 nm (excitation)/600 nm (emission).

The morphology of the cells and their expansion were assessed through staining of F-actin filaments with Alexa Fluor 594-phalloidin (Invitrogen) to visualize the cytoskeleton and cell nuclei with DAPI. Briefly, cells were fixed by incubating with 4% (w/v) paraformaldehyde for 15 min, then permeabilized using 0.3% (v/v) Triton in DPBS for 10 min and blocked with 1% (w/v) bovine serum albumin (BSA) in DPBS for 30 min at room temperature. Samples were serially incubated with phalloidin (1:400 dilution in 0.1% BSA) and DAPI (1:1000 dilution) solution for 45 min and 1 min, respectively. The samples were washed and imaged using the Zeiss fluorescence microscope.

#### 4.4.13 | *In vivo* studies on GelPatch and GelPatch+MC

All the *in vivo* studies were approved by the IACUC (protocol 2018-076-01C) at University of California Los Angeles (UCLA). Male Wistar rats (200–250 g) were purchased from Charles River Laboratories (Boston, MA, USA). Anesthesia was achieved by inhalation of isoflurane (2–2.5%), followed by subcutaneous meloxicam administration (5 mg/kg). After anesthesia, 81-cm incisions were made on the dorsal skin of rats, and small subcutaneous pockets were made using a blunt scissor. GelPatch+MC, as well as pristine GelPatch as a control were formed using a cylindrical compression mold and then were lyophilized. The lyophilized hydrogels were sterilized under UV light for 10 min. The sterile hydrogels were then implanted into the subcutaneous pockets, and incisions were closed with 4-0 polypropylene sutures (AD Surgical). At day 7 and 28 post-implantation, the rats were euthanized, and the hydrogels were explanted with the surrounding tissues for histological assessment.

Histological analyses were performed on the explanted hydrogels to investigate the inflammatory responses caused by the implanted hydrogels. After explantation of the samples with the surrounding tissues, they were fixed in 4% (v/v) paraformaldehyde for 4 h and incubated in 15% and 30% sucrose, respectively (at 4°C, overnight). Samples were then embedded in Optimal Cutting Temperature compound (OCT), frozen in liquid nitrogen, and sectioned by using Leica CM1950 cryostat machine. Sections (8  $\mu$ m thickness) were mounted

on positively charged glass slides using DPX mountant (Sigma) for Hematoxylin and Eosin (H&E) staining and Masson's Trichrome (MT) staining, and ProLong™ Gold antifade reagent (Thermo fisher scientific) for immunofluorescence (IF) staining. The slides were then processed for H&E and MT staining (Sigma) according to manufacturer instructions. IF staining was also performed on mounted samples as previously reported. Anti-CD68 (ab125212) (Abcam) was used as primary antibody, and Goat-anti Rabbit IgG (H + L) secondary antibody conjugated to Alexa Fluor® 594 (Invitrogen) was used as a detection reagent. All samples were then stained using 4',6-diamidino-2-phenylindole (DAPI) and the imaging was performed using ZEISS Axio Observer Z1 inverted microscope.

#### 4.4.14 | Statistical analysis

Results were presented as means ± SD (\* $p < 0.05$ , \*\* $p < 0.01$ , \*\*\* $p < 0.001$ , and \*\*\*\* $p < 0.0001$ ). One-way or two-way analysis of variance (ANOVA) was performed for statistical analysis (GraphPad Prism 8.0).

#### AUTHOR CONTRIBUTIONS

**Xi Chen:** Conceptualization (equal); data curation (equal); formal analysis (equal); writing – original draft (lead); writing – review and editing (equal). **Shima Gholizadeh:** Conceptualization (lead); data curation (lead); formal analysis (lead); writing – original draft (lead); writing – review and editing (equal). **Mahsa Ghovvati:** Data curation (supporting); formal analysis (supporting); writing – review and editing (supporting). **Ziqing Wang:** Data curation (supporting); formal analysis (supporting); writing – review and editing (supporting). **Azadeh Mostafavi:** Data curation (supporting); formal analysis (supporting); writing – review and editing (supporting). **Reza Dana:** Conceptualization (supporting); supervision (supporting); writing – original draft (supporting); writing – review and editing (supporting). **Nasim Annabi:** Conceptualization (equal); funding acquisition (lead); project administration (lead); resources (lead); supervision (lead); writing – original draft (equal); writing – review and editing (equal).

#### ACKNOWLEDGMENTS

This work is supported by Department of Defense Vision Research Program Technology/Investigator-Initiated Research Award (W81XWH-21-1-0869), and the National Institutes of Health (NIH) (R01EB023052).

#### CONFLICT OF INTEREST STATEMENT

N.A. and R.D. hold equity in GelMEDIX Inc.

#### DATA AVAILABILITY STATEMENT

All data needed to evaluate the conclusions in the article is present in the article and/or the Supporting Information. Additional data related to this article may be requested from the authors.

#### ORCID

Mahsa Ghovvati  <https://orcid.org/0000-0002-0608-5768>

Nasim Annabi  <https://orcid.org/0000-0003-1879-1202>

#### REFERENCES

- Occhiutto ML, Freitas FR, Maranhao RC, Costa VP. Breakdown of the blood-ocular barrier as a strategy for the systemic use of nanosystems. *Pharmaceutics*. 2012;4(2):252-275. doi:10.3390/pharmaceutics4020252
- Gholizadeh S, Wang Z, Chen X, Dana R, Annabi N. Advanced nanodelivery platforms for topical ophthalmic drug delivery. *Drug Discov Today*. 2021;26(6):1437-1449.
- Cao Y, Samy KE, Bernards DA, Desai TA. Recent advances in intraocular sustained-release drug delivery devices. *Drug Discov Today*. 2019;24(8):1694-1700. doi:10.1016/j.drudis.2019.05.031
- Cooper RC, Yang H. Hydrogel-based ocular drug delivery systems: emerging fabrication strategies, applications, and bench-to bedside manufacturing considerations. *J Control Release*. 2019;306:29-39.
- Franco P, De Marco I. Contact lenses as ophthalmic drug delivery systems: a review. *Polymers (Basel)*. 2021;13(7):1102. doi:10.3390/polym13071102
- Thakur Singh RR, Tekko I, McAvoy K, McMillan H, Jones D, Donnelly RF. Minimally invasive microneedles for ocular drug delivery. *Expert Opin Drug Deliv*. 2017;14(4):525-537. doi:10.1080/17425247.2016.1218460
- Pimenta AFR, Serro AP, Paradiso P, Saramago B, Colaço R. Diffusion-based design of multi-layered ophthalmic lenses for controlled drug release. *PLoS One*. 2016;11(12):e0167728. doi:10.1371/journal.pone.0167728
- Alió JL, Mulet ME, Garcia JC. Use of cyanoacrylate tissue adhesive in small-incision cataract surgery. *Ophthalmic Surg Lasers*. 1996;27(4):270-274.
- Trott AT. Cyanoacrylate tissue adhesives: an advance in wound care. *JAMA*. 1997;277(19):1559-1560. doi:10.1001/jama.1997.03540430071037
- Ciapetti G, Stea S, Cenni E, et al. Cytotoxicity testing of cyanoacrylates using direct contact assay on cell cultures. *Biomaterials*. 1994;15(1):63-67. doi:10.1016/0142-9612(94)90199-6
- Bhatia SS. Ocular surface sealants and adhesives. *Ocul Surf*. 2006;4(3):146-154. doi:10.1016/s1542-0124(12)70041-1
- Yañez-Soto B, Liliensiek SJ, Murphy CJ, Nealey PF. Biochemically and topographically engineered poly(ethylene glycol) diacrylate hydrogels with biomimetic characteristics as substrates for human corneal epithelial cells. *J Biomed Mater Res A*. 2013;101(4):1184-1194. doi:10.1002/jbm.a.34412
- ReSure Sealant. PMA P130004: FDA Summary of Safety and Effectiveness. 2014.
- Masket S, Hovanesian JA, Levenson J, et al. Hydrogel sealant versus sutures to prevent fluid egress after cataract surgery. *J Cataract Refract Surg*. 2014;40(12):2057-2066. doi:10.1016/j.jcrs.2014.03.034
- Trujillo-de Santiago G, Sharifi R, Yue K, et al. Ocular adhesives: design, chemistry, crosslinking mechanisms, and applications. *Biomaterials*. 2019;197:345-367.
- Sani ES, Kheirkhah A, Rana D, et al. Sutureless repair of corneal injuries using naturally derived bioadhesive hydrogels. *Sci Adv*. 2019;5(3):eaav1281. doi:10.1126/sciadv.aav1281
- Jumelle C, Yung A, Sani ES, et al. Development and characterization of a hydrogel-based adhesive patch for sealing open-globe injuries. *Acta Biomater*. 2022;137:53-63. doi:10.1016/j.actbio.2021.10.021
- Coffey MJ, Decory HH, Lane SS. Development of a non-settling gel formulation of 0.5% loteprednol etabonate for anti-inflammatory use as an ophthalmic drop. *Clin Ophthalmol*. 2013;7:299-312. doi:10.2147/oph.S40588
- Nabar GM, Mahajan KD, Calhoun MA, et al. Micelle-templated, poly(lactic-co-glycolic acid) nanoparticles for hydrophobic drug delivery. *Int J Nanomed*. 2018;13:351-366. doi:10.2147/IJN.S142079

20. Hussein YHA, Yousry M. Polymeric micelles of biodegradable diblock copolymers: enhanced encapsulation of hydrophobic drugs. *Materials (Basel)*. 2018;11(5):688. doi:10.3390/ma11050688
21. Chan PS, Xian JW, Li Q, Chan CW, Leung SSY, To KKW. Biodegradable thermosensitive PLGA-PEG-PLGA polymer for non-irritating and sustained ophthalmic drug delivery. *AAPS J*. 2019;21(4):59. doi:10.1208/s12248-019-0326-x
22. Rijcken CJF, Veldhuis TFJ, Ramzi A, Meeldijk JD, van Nostrum CF, Hennink WE. Novel fast degradable thermosensitive polymeric micelles based on PEG-block-poly(N-(2-hydroxyethyl)methacrylamide-oligolactates). *Biomacromolecules*. 2005;6(4):2343-2351. doi:10.1021/bm0502720
23. Mandal A, Bisht R, Rupenthal ID, Mitra AK. Polymeric micelles for ocular drug delivery: from structural frameworks to recent preclinical studies. *J Control Release*. 2017;248:96-116.
24. Özsoy Y, Güngör S, Kahraman E, Durgun ME. Polymeric micelles as a novel carrier for ocular drug delivery. *Nanoarchitectonics Biomedicine*. 2019;85-117. doi:10.1016/B978-0-12-816200-2.00005-0
25. Talelli M, Rijcken CJF, Lammers T, et al. Superparamagnetic iron oxide nanoparticles encapsulated in biodegradable thermosensitive polymeric micelles: toward a targeted nanomedicine suitable for image-guided drug delivery. *Langmuir*. 2009;25(4):2060-2067. doi:10.1021/la8036499
26. Soga O, van Nostrum CF, Fens M, et al. Thermosensitive and biodegradable polymeric micelles for paclitaxel delivery. *J Control Release*. 2005;103(2):341-353. doi:10.1016/j.jconrel.2004.12.009
27. Tempest-Roe S, Joshi L, Dick AD, Taylor SR. Local therapies for inflammatory eye disease in translation: past, present and future. *BMC Ophthalmol*. 2013;13(1):39. doi:10.1186/1471-2415-13-39
28. Alberth M, Wu W-M, Winwood D, Bodor N. Lipophilicity, solubility and permeability of loteprednol etabonate: a novel, soft anti-inflammatory steroid. *Aust J Biol Sci*. 1991;2(2):115-125.
29. Talelli M, Iman M, Varkouhi AK, et al. Core-crosslinked polymeric micelles with controlled release of covalently entrapped doxorubicin. *Biomaterials*. 2010;31(30):7797-7804. doi:10.1016/j.biomaterials.2010.07.005
30. Shi Y, van der Meel R, Theek B, et al. Complete regression of xenograft tumors upon targeted delivery of paclitaxel via II-II stacking stabilized polymeric micelles. *ACS Nano*. 2015;9(4):3740-3752. doi:10.1021/acsnano.5b00929
31. van Hasselt PM, Janssens GE, Slot TK, et al. The influence of bile acids on the oral bioavailability of vitamin K encapsulated in polymeric micelles. *J Control Release*. 2009;133(2):161-168. doi:10.1016/j.jconrel.2008.09.089
32. Naksuriya O, Shi Y, van Nostrum CF, Anuchapreeda S, Hennink WE, Okonogi S. HPMA-based polymeric micelles for curcumin solubilization and inhibition of cancer cell growth. *Eur J Pharm Biopharm*. 2015;94:501-512. doi:10.1016/j.ejpb.2015.06.010
33. Crielaard BJ, Rijcken CJ, Quan L, et al. Glucocorticoid-loaded core-cross-linked polymeric micelles with tailorable release kinetics for targeted therapy of rheumatoid arthritis. *Angew Chem Int Ed Engl*. 2012;51(29):7254-7258. doi:10.1002/anie.201202713
34. Kim SH, Tan JPK, Nederberg F, et al. Hydrogen bonding-enhanced micelle assemblies for drug delivery. *Biomaterials*. 2010;31(31):8063-8071. doi:10.1016/j.biomaterials.2010.07.018
35. Kogan G, Soltés L, Stern R, Gemeiner P. Hyaluronic acid: a natural biopolymer with a broad range of biomedical and industrial applications. *Biotechnol Lett*. 2007;29(1):17-25. doi:10.1007/s10529-006-9219-z
36. Campbell PK, Bennett SL, Driscoll A, Sawhney AS. *Evaluation of Absorbable Surgical Sealants: In vitro Testing*. Confluent Surgical, Inc.; 2005.
37. Spotnitz WD. Fibrin Sealant: the only approved hemostat, Sealant, and adhesive—a laboratory and clinical perspective. *ISRN Surg*. 2014;2014:203943. doi:10.1155/2014/203943
38. Bagheri M, Bresseleers J, Varela-Moreira A, et al. Effect of formulation and processing parameters on the size of mPEG-b-p(HPMA-Bz) polymeric micelles. *Langmuir*. 2018;34(50):15495-15506. doi:10.1021/acs.langmuir.8b03576
39. Bencherif SA, Srinivasan A, Horkay F, Hollinger JO, Matyjaszewski K, Washburn NR. Influence of the degree of methacrylation on hyaluronic acid hydrogels properties. *Biomaterials*. 2008;29(12):1739-1749.
40. Ghovvati M, Baghdasarian S, Baidya A, Dhal J, Annabi N. Engineering a highly elastic bioadhesive for sealing soft and dynamic tissues. *J Biomed Mater Res B Appl Biomater*. 2022;110(7):1511-1522.
41. Mostafavi A, Samandari M, Karvar M, et al. Colloidal multiscale porous adhesive (bio)inks facilitate scaffold integration. *Appl Phys Rev*. 2021;8(4):041415.
42. Baghdasarian S, Saleh B, Baidya A, et al. Engineering a naturally derived hemostatic sealant for sealing internal organs. *Mater Today Bio*. 2022;13:100199.
43. Shirzaei Sani E, Portillo-Lara R, Spencer A, et al. Engineering adhesive and antimicrobial hyaluronic acid/elastin-like polypeptide hybrid hydrogels for tissue engineering applications. *ACS Biomater Sci Eng*. 2018;4(7):2528-2540. doi:10.1021/acsbomaterials.8b00408

## SUPPORTING INFORMATION

Additional supporting information can be found online in the Supporting Information section at the end of this article.

**How to cite this article:** Chen X, Gholizadeh S, Ghovvati M, et al. Engineering a drug eluting ocular patch for delivery and sustained release of anti-inflammatory therapeutics. *AIChE J*. 2023;69(6):e18067. doi:10.1002/aic.18067